약학석사 학위논문

대식세포의 움직임을 조절하는 Lysyl-tRNA Synthetase (KRS)의 기전 연구

The Mechanism of Lysyl-tRNA Synthetase (KRS) in the Control of Macrophage Migration

2017 년 8 월

서울대학교 융합과학기술대학원

분자의학 및 바이오제약학과 의약생명과학전공

김 건 호

대식세포의 움직임을 조절하는

Lysyl-tRNA Synthetase (KRS)의 기전 연구

The Mechanism of Lysyl-tRNA Synthetase (KRS)

in the Control of Macrophage Migration

지도교수 김 성 훈

이 논문을 약학석사 학위논문으로 제출함

2017 년 7 월

서울대학교 융합과학기술대학원
분자의학 및 바이오제약학과 의약생명과학전공
김 건 호

김건호의 약학석사 학위논문을 인준함
2017 년 7 월

위 원 장 _____(인)

부 위 원 장 _____(인)

위 원 _____(인)

ABSTRACT

Over the past few years, knowledge in immunology has been emphasized for the development of novel drugs, because inflammatory responses are deeply involved in life-threatening pathological human diseases unless seemingly unrelated. Although appropriate infiltration of distinct immune cells plays a central role in protecting against pathogens, aberrant trafficking signals by excessive immune responses drive multifactorial pathogenesis. Therefore, the control of immune cell migration has been risen a novel target for treating various human diseases including cardiovascular diseases.

In our previous study, non-canonical function of lysyl-tRNA synthetase (KRS), one of aminoacyl-tRNA synthetase (ARSs), was regarded as an important cancer cell regulator in that KRS translocates to the plasma membrane on laminin (LN) signal, inducing cell migration. However the role of KRS in immune cells is not well understood yet. Here, we demonstrated that KRS plays a crucial role in the progression of pathogenesis via the control of macrophage migration *in vitro* and *in vivo* studies. Although translocation of KRS to the plasma membrane in RAW 264.7 cells on LN 421 signal induced macrophage recruitment, the small compound BC-KI-00053, KRS inhibitor, showed a significant decreases in macrophage migration and ameliorated the progression of disease in rat models. Through this work, we provided a molecular basis for better understanding of novel functions of KRS, not only as an important regulator of macrophage migration but also as an effective therapeutic target for human pathologies in the

near future.

Key Words : Lysyl-tRNA synthetase (KRS), macrophage, migration, inhibition, laminin, Pulmonary Arterial Hypertension (PAH)

Student ID: 2015-26071

CONTENTS

LIST OF FIGURES

ABBREVIATION LIST

KRS: Lysyl-tRNA synthetase

MSC: Multi-tRNA synthetase complex

ECM: Extracellular matrix

LN: Laminin

Col: Collagen

FN: Fibronectin

LPS: Lipopolysaccharides

PAH: Pulmonary Arterial Hypertension

RVSP: Right Ventricular Systolic Pressure

FDA: Food and Drug Administration

CCK8: Cell Counting Kit-8

MCT: Monocrotaline

INTRODUCTION

In recent, many attentions on the field of immunity have been burgeoning due to the high potential in the field of drug development, and infiltration of leukocytes is one of the key factors involved in the diseases induction and worsening as well as pathological tissue remodeling (1). Hypertension- and fibrosis-related diseases can be good examples to show the relationship between leukocyte infiltration and disease development in that immune cell infiltration in the damaged tissues exacerbates the positive feedback among inflammation, tissue damage, fibrosis and high blood pressure.

According to the reports from World Health Organization, cardiovascular disease is the single largest cause of death worldwide and pulmonary arterial hypertension (PAH) is one of the cardiovascular diseases, which has no effective drugs to enhance survival rate without side effects (2). PAH is a severe, life-threatening disease and pathologic condition in which pulmonary arterial pressure exceeds 25 mmHg at rest (2). Right heart dysfunction by elevation in pulmonary vascular resistance is known to be the main cause of death for PAH (3). Recent cohorts analysis of patients with PAH has revealed that the mortality rate for PAH is increasing because of the difficulties in diagnosis as well as side effects of drugs for PAH (4). According to the recent analysis of immune reaction in PAH, dysregulated immune responses are known to critical contributors leading aberrant pulmonary vascular remodeling through excessive migration and proliferation of vascular cells including endothelial cells and smooth muscle cells. Infiltration of

leukocytes induces the secretion of cytokines and chemokines through endothelial cells, leading to the hypertrophy and proliferation of smooth muscle cells in pathogenic conditions (5). Although dysfunction of immune response is correlated with the severity of the syndrome through the imbalance of pulmonary vascular remodeling, the detailed mechanisms remain unclear (6).

Inflammation by infiltration of immune cells in tissue is known as a key cause of the disease, and the role of macrophage is tightly related to the progression of PAH. It is known that excessive recruitment of macrophage contributes to endothelial cell death in vascular regression and the development of plexiform lesions around occluded arterioles is implicated in PAH (7). In addition, macrophages have been predominantly observed in experimental and clinical PAH, and depletion of CD 68+ macrophage prevents PAH *in vivo* model (8). Thus, inhibition of macrophage infiltration could be a pivotal key to alleviate the symptoms of PAH.

As shown in the list of FDA approved therapies for PAH, predominant treatments are just focusing on dilating the occluded vessels without removing the cause of PAH, calling attention for the desperate need of mechanism-based therapeutics (9). Despite the efforts to identify drugs for PAH, the mechanism underlying the development of PAH is still obscure. Many factors such as adhesion molecules and extracellular matrix (ECM) involve in the migration of immune cells. The accumulation of extracellular matrix (ECM) components including laminin results in immune cell migration in vascular remodeling, and the decomposition of laminin is a representative pathological feature observed in PAH patients (10). However, what type of laminin subtypes is important for the PAH-

related immune cell infiltration and which molecules respond to laminin in this context have not been fully studied yet. While laminin α4 located around the vascular basement membrane specifically recruits immune cells (11), the exact role of laminin and related molecules are still unclear, compared to the deep knowledge of various cytokines in PAH (12).

Aminoacyl-tRNA synthetases (ARSs), ligating amino acids to their cognate tRNAs for high translational fidelity of genetic information, are critical for protein synthesis and cell survival (13). Recent studies have revealed that the abnormal expressions of ARSs are significant to the progression of various diseases in pathological condition (14). Lysyl-tRNA synthetase (KRS) is one of the ARSs whose levels are highly upregulated in various cancers. KRS is translocated from multi-tRNA synthetase complex (MSC) to plasma membrane on laminin signal and enhances cancer metastasis (15, 16). Because the interaction of 67 laminin receptor (67LR) and membranous KRS promotes cancer metastasis, inhibition of two molecules effectively controls metastasis, and YH 16899 was selected through yeast two-hybrid (Y2H) assay (16). To improve its efficacy and stability, we set up a migration assay with newly synthesized derivatives of YH 16899, and we eventually chose BC-KI-00053 as a finalized KRS inhibitor.

While the role of KRS as a potent regulator for the cancer cell migration is relatively well defined, there was little information for the effect of KRS on the migration of other cell types (14). Here, we demonstrated that KRS promotes macrophage migration in LN 421-dependent manner and induced the translocation of KRS to the plasma membrane in RAW 264.7 cells. We also proved that compound BC-KI-00053, which inhibits the KRS-dependent cancer cell migration,

also efficiently decreased the level of membranous KRS, reducing the migration of RAW 264.7 cells. Finally, we confirmed that BC-KI-00053 significantly relieved the symptoms of PAH *in vivo* model. This study strongly suggests KRS as a potent target for the inhibition of macrophage migration, and also KRS inhibitor as a promising therapeutic strategy for PAH treatment.

MATERIALS AND METHODS

Cell cultures and materials

RAW 264.7 cells were purchased from KCLB (Korean cell line bank) and were cultured in Dulbecco's modified Eagle's medium (DMEM) (with 4500 mg/L Glucose, 400mg/L Glutamine, Sodium pyruvate, Hyclone, Cat # 30243.01) supplemented with 10 % fetal bovine serum (FBS, Hyclone) and 1 % penicillin and streptomycin at 37 ^{o}C in 5 % CO_2 humidified incubator.

RNA interference

Transfection was performed according to the manufacturer's instructions. Each si-RNA and Lipofectamin 2000 (Invitrogen, Cat # 11668-019) mixture was incubated for 15 minutes in serum free media. After vortexing the mixture, it is added to each well and further incubated for 48-72 hours for the knockdown of target gene in cells. Si-RNA duplex with medium GC content (Invtrogen, Cat # 12935-300) was used as a negative control in each experiment. Primer sequences for si-RNA were as follows; si-KRS: AGAAGUUCUCGU CUAUGAACAUGG C, si-LRS: UUUGGAAUCAGAUCCUUGCCAGAGG

Immunoblotting

After harvest, cells were lysed in cold lysis buffer (50 mM Tris-HCL (pH 7.5), 150 mM NaCl, 5 mM EDTA, 1 % NP-40), supplemented with protease inhibitor (Calbiochem, Cat # 535140) and phosphatase inhibitor (Thermo Scientific,

Cat # 78427) for 30 minutes at 4^{o}C. Then, the extracts were centrifuged with 13,000 rpm for 15 minutes at 4 ^{o}C.

The supernatant proteins were quantified by Bradford assay (Biorad, Cat # 500-0006). Sample buffer (5X) containing bromophenol blue (0.25 %), dithiothreitol (0.5 M), glycerol (20 %), and sodium dodeyl sulfate (10 %) and lysis buffer were added to quantify the final samples for equal concentration.

After boiling samples for 10 minutes at 100^{o}C, samples were loaded on SDS-PAGE gels and electrophoresis was performed. The gel was transferred to polyvinylidenefloride (PVDF) membranes (Milipore, Cat # IPVH 00010) at 55 mA, 6V for 90 minutes (BioRad Cat. Powerpac 3000). The membranes were incubated with 0.3 % TBS-T containing 5 % skim milk for 1 hour to prevent non-specific bindings. After blocking, primary antibodies were added to the membrane and incubated overnight at 4^{o}C. After washing with 0.3 % TBS-T 4 times for 5 minutes respectively, secondary antibodies were added to membranes and incubated for 60 minutes at room temperature. After washing according to the same procedure mentioned above, ECL solution (Santacruz biotechnology, Cat # Sc-2048, GE healthcare life sciences, Cat # RPN2232) was applied to the membrane to detect the protein of interest.

Cell migration assay

Migration assays were performed as described in elsewhere (12) with minor modification. Cell migration was determined by using 24-well Boyden chambers with polycarbonate membrane (5.0-μm pore size, Corning). Gelatin (0.5 mg/ml) in PBS was coated onto the membrane of transwell and the membrane was

dried for 2 hours. Suspended RAW 264.7 cells in serum-free DMEM were added to the upper chamber at 1 x 10^5 cells per each well. Laminin (10 μg/ml), fibronectin (10 μg/ml), collagen (10 μg/ml), and laminin subtypes (1 μg/ml) were placed in lower well, and the cells were allowed to migrate to the underside of the porous membrane for 24 hours at 37°C in a CO_2. The cells were then fixed with 70% methanol in H_2O for 30 minutes and washed with PBS twice. The cells were stained with 50 % hematoxylin (sigma Cat # HHS32) in H_2O for 30 minutes and washed with PBS twice again. After nonmigrant cells were removed from the upper face of the membrane with a cotton swab. The membranes were excised from the chamber and mounted. 3 random image of the migrant cells were counted in the microscope (x 20)

Immunohistochemistry

Dissected lung tissues embedded in paraffin were prepared for the section at 6-μm thickness. Autostainer was used according to the manufacture's instruction. Briefly, the section of each lung tissue was stained in xylene 3 times for 5 minutes, and washed with 100 % ethanol for 2 minutes, 95 % ethanol for 2 minutes, 90 % ethanol for 2 minutes, 70 % ethanol for 2 minutes, distilled water for 2 minutes, and PBS for 2 minutes respectively. After treatment of 0.3 % H_2O_2, the samples were washed with PBS twice for 5 minutes. After heating in the microwaeve in the 0.01 M citrate buffer, the slides were washed with PBS-T (0.03 %), and then incubated with 2 % goat serum in 2 % BSA for 30 minutes to prevent non-specific binding. Anti-CD 68 antibody (1:200) was applied onto the tissue overnight at 4°C. After washing with PBS-T 5 minutes for 3 times, the samples were completely

covered by polymer-HRP anti-mouse (DAKO, Cat # P0447) at 4^{o}C for 1 hour. After washing with PBS-T 3 times, the mixture of DAB, substrate buffer was added to the sample for the detection of interest. The stained tissue was treated by hematoxylin (sigma, Cat # HHS32) for 1 minute and then treated in 70 % ethanol for 2 minutes, 90 % ethanol for 2 minutes, 95 % ethanol for 2 minutes, 100 % ethanol twice for 2 minutes, and xylene three times for 5 minutes. Each sample was mounted to visualize the staining of the slides

Cytokine array

Rat cytokine array (R&D systems Cat # ARY008) was performed to investigate the expression of 29 cytokines and chemokines, following the manufacturer's protocol. Enough amounts of serum of monocroatine (MCT)-induced rat, and each of the groups treating BC-KI-00053 (25 mg/kg, 50 mg/kg), and sildenafil (25 mg/kg) were prepared before starting experiment. While blocking the each membrane for 1 hour on the rocking shaker at room temperature, appropriate amounts of serum sample containing detection antibody cocktail were prepared. After washing 3 times, incubated the membrane with serum/antibody mixture overnight at 4^{o}C on rocking shaker. After washing 3 times for 10 minutes, diluted Streptavid-HRP was added to the each membrane and incubated for 30 minutes at room temperature. After washing 3 times, drained off all the washing buffer from the membrane and Chemi Reagent Mix was added onto membrane for 1 minute to expose the membrane to X-ray film.

Cell viability

The viability of RAW 264.7 cells was evaluated using Cell Counting Kit-8 (CCK-8) assay (Dojindo Laboratories, Kumamoto, Japan). RAW 264.7 cells were seeded in 96-wel plate at a density of 2.0 x 10^4 cells per well for 24 hours in DMEM containing 10 % FBS and 100 µg/ml Penicillin/ streptomycin and indicated concentration of BC-KI-00053 was added to each well containing 2 % FBS media for additional 24 hours. After adding 10 µl of CCK-8 reagent to each well, incubated 2 hours until colorimetric change occurs. The optical density (O.D) was measured at 450 nm using microplate reader (Bio-Rad Laboratories, USA) to determine the proliferation of RAW 264.7 cells

RESULTS

Migration of macrophage is specifically triggered by LN 421

Since prominent infiltrated macrophages and temporal change in the deposition of ECM were reported in the plexiform lesions occluded arterioles in PAH patient, it is important to investigate which ECM components mainly contributes to the migration of macrophage in the progression of PAH. Therefore, the equal concentration of ECM components (laminin, fibronectin, and collagen) was used *in vitro* transwell migration assay to investigate the effect of the ECM component on the monocyte cell migration. Interestingly, only laminin, but not the other ECM component, enhanced the cell migration as shown in the cell staining image and quantitated graph (Fig 1A, 1B). It demonstrates that laminin is the main ECM component triggering the migration of macrophage.

Because genetically different 15 isoforms of laminin have been identified with distinct functional role, we evaluated the effect of each laminin subtype (1 μg/ml) on cell migration, and confirmed that LN 421 specifically stimulated the migration of RAW 264.7 cells (Fig 1C, 1D). Since these results show that LN 421 can be the major inducer of macrophage migration and KRS is known as the key responder under laminin signaling (15), we further investigated the relationship between LN 421 and KRS for the macrophage migration.

KRS modulates LN 421-dependent migration of macrophage

In the previous study, cell migration was strengthened via expression of

KRS on laminin signal (15). Therefore, we determined the effect of KRS on cell migration using knockdown and upregulation of KRS. Cell migration assay with the silencing of KRS and LRS by si-RNA transfection was performed to monitor their effect on migration, and the quantified graph exhibited approximately 70 % reduction when KRS level was silenced (Fig 2A). Knockdown of LRS did not affect the migration level of RAW 264.7 cells implying that cell migration is specifically influenced by KRS. In the same context, overexpression of KRS dramatically increased the cell migration, but overexpression of LRS hardly affected to the cell migration as shown in EV-transfected cells (Fig 2B). This result strongly verified that cell migration dependent upon LN 421 is tightly correlated with KRS, but not LRS.

LN 421 signal induces the translocation of KRS to plasma membrane

Because association of cancer cell migration and translocation of KRS from cytosol to plasma membrane in the presence of laminin has been reported in the previous study, we also confirmed the effect of LN 421 on cellular location of KRS in RAW 264. 7 cells. To confirm the cellular localization of KRS on LN 421 signal, RAW 264.7 cells were fractionized into cytosol and plasma membrane and we investigated the level of KRS in the absence and presence of LN 421. Localization of KRS to plasma membrane via LN 421 signal was confirmed in a time dependent manner, even though the majority of KRS still remained in the cytosol (Fig 3A). This result is productive to support that translocation of KRS is a significant mechanism in the control of macrophage migration.

KRS inhibitor (BC-KI-00053) attenuates LN 421-dependent migration of macrophage

Because the result above supported the hypothesis that inhibition of KRS leads to reduction in cell migration, we performed migration assay with the treatment of KRS inhibitor. To test the efficacy of KRS inhibitor (BC-KI-00053) in cell migration *in vitro*, concentrations of BC-KI-00053 at 0 nM, 30 nM, 100 nM, 300 nM, 1 μM, and 3 μM were treated in the transwells. Eventually, BC-KI-00053 effectively reduced the number of migrating cells compared with the non-treated control group (Fig 4A), and numerical bar graph presented showed that BC-KI-00053 significantly blocked the macrophage migration from 300 nM with IC_{50} value of 58.81 nM (Fig 4B, 4C).

In addition, we analyzed the viability of the cells treated with BC-KI-00053 to confirm that the dramatic effect on migration was not due to the cytotoxicity of the compound. The result shows that BC-KI-00053 treatment under the same condition with migration assay did not exert any cytotoxicity in RAW 264.7 cells (Fig 4D). All together, these results strongly demonstrated that BC-KI-00053 sufficiently inhibits the migration of macrophage without any adverse effects on RAW 264.7 cells.

BC-KI-00053 suppresses LN 421-mediated membrane localization of KRS

Based on the significant inhibitory effect of BC-KI-00053 on the macrophage migration, we hypothesized that KRS inhibitor would affect the level of membranous KRS in RAW 264.7 cells, since BC-KI-00053 reduces cancer cell metastasis via decreasing the level of KRS in the cell membrane hindering the pro-

migratory signaling cascades. For further validation of cellular location of KRS *in vitro* by BC-KI-00053, we fractionated cellular proteins of RAW 264.7 cells into cytosolic and membrane portions after treating 100 nM BC-KI-00053, and observed that the level of membranous KRS was dramatically reduced by BC-KI-00053 treatment (Figure 5A). These results indicate that downregulation of macrophage migration shown in Figure 4A is tightly correlated with the reduction in KRS level in plasma membrane. Therefore, it is suggested that the level of KRS in the plasma membrane is critical for the control of macrophage migration.

BC-KI-00053 relieves the symptoms of PAH *in vivo*

Next, we evaluated the efficacy of BC-KI-00053 *in vivo* in comparison with sildenafil, an FDA-approved anti-PAH drug. The scheme of experimental design is presented in Fig 6A. All of rats was treated with MCT (60 mg/kg) at day 0 and then they were administered by the oral route with vehicle, BC-KI-00053 (25 mg/kg and 50 mg/kg), and sildenafil (25 mg/kg), respectively every day for 3 weeks (Fig 6A). Based on the immunohistochemistry analysis, BC-KI-00053-treated group revealed a dose dependent decrease of macrophage infiltration in the lung tissue, and also showed better inhibitory effect on macrophage infiltration than sildenafil-administrated group (Fig 6B). In addition, cytokine array was performed to determine the change in pivotal molecules in PAH, and L-selectin and Rantes, which are known as markers for PAH (19, 20), were significantly reduced in BC-KI-00053 group in a dose dependent manner (Fig 6C). The accurate assessment of right ventricular systolic pressure (RVSP), utilized as an important marker for PAH, indicated that BC-KI-00053-administrated group notably reduced

RVSP more effectively than sildenafil (Fig 6D). According to Table 1, however, there is no meaningful change in cardiac output in each group compared to dramatic change in RVSP *in vivo* model. Combined together, these results proved that BC-KI-00053 could not only reduce the macrophage migration *in vivo* but also alleviate PAH symptoms, suggesting that KRS would be a potentially novel and potent target to treat PAH.

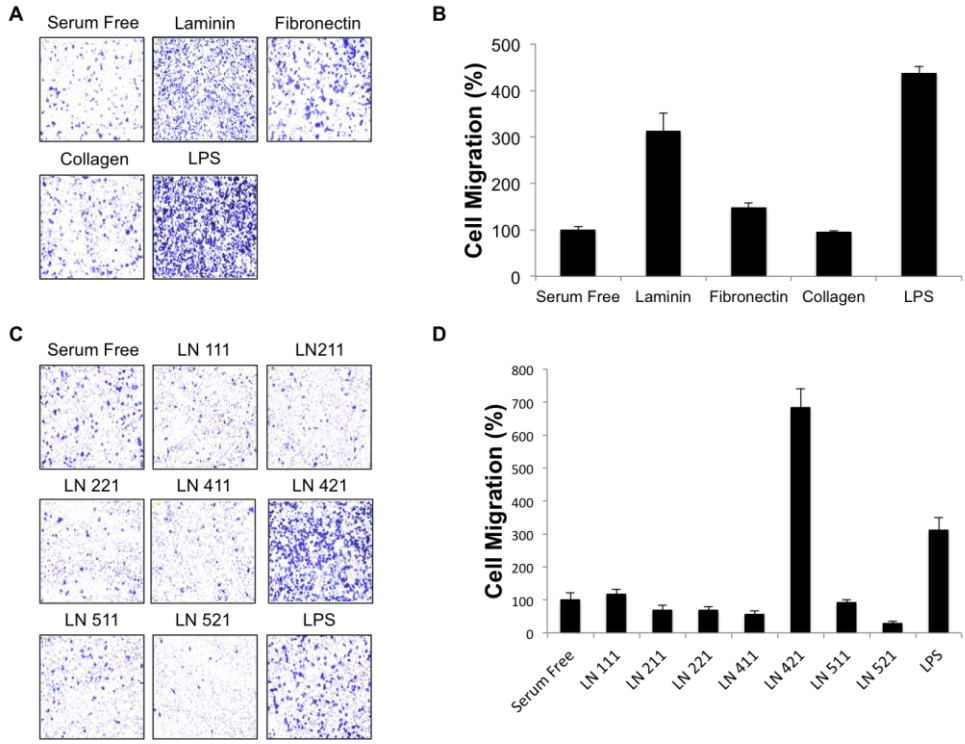

Figure 1. Migration of macrophage is specifically triggered by LN 421

(A) RAW 264.7 cells (1 x 10^5/well) and equal concentration (10 μg/ml) of ECM components including laminin (LN), fibronectin (FN), and collagen (Col), were added to the upper and lower wells of transwell chamber coated with gelatin, respectively, and the cells migrated through the membrane were detected by the hematoxylin staining as described in *Materials and Methods*. 100 ng/ml of Lipopolysaccharides (LPS) was used as a positive control.

(B) The results from (A) were counted (x 10) in 3 random fields (mean ± SD, n = 3), and numerical data was presented as bar graphs.

(C) RAW 264.7 cells were loaded onto the upper well, and different isoforms of each laminin (1 μg/ml) were added to the lower well and allowed the cells to penetrate transwsell membrane.

(D) The cells migrating through the membrane were counted as above.

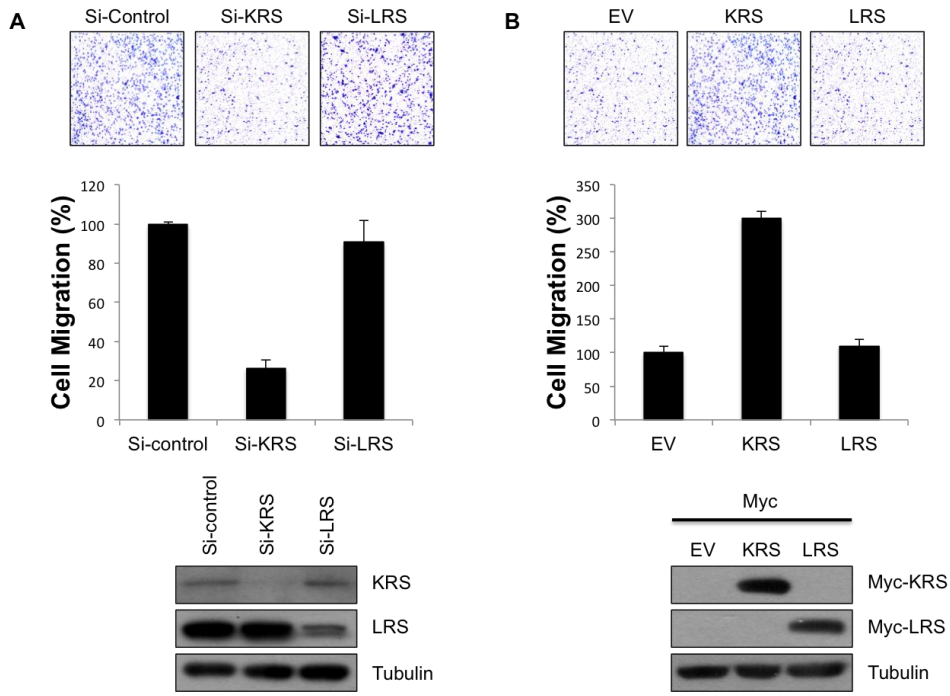

Figure 2. KRS modulates LN 421-dependent migration of macrophages

(A) The effect of KRS on the migration of RAW 264.7 cells was determined with knockdown of KRS and LRS was used as one of ARSs control. To observe the effect of cell migration by KRS, its specific si-RNA was used. Migration rates were quantified by counting the migrated cells in 3 random fields under a light microscope (mean ± SD, n = 3). Cell lysates were analyzed by immunoblotting.

(B) RAW 264.7 cells were transfected with Myc-KRS, Myc-LRS, and Myc-EV (empty vector) for 24 hours and migration assay was performed as described in *Materials and Methods* (mean ± SD, n = 3). The level of overexpressed Myc-KRS and Myc-LRS was detected by immunoblotting.

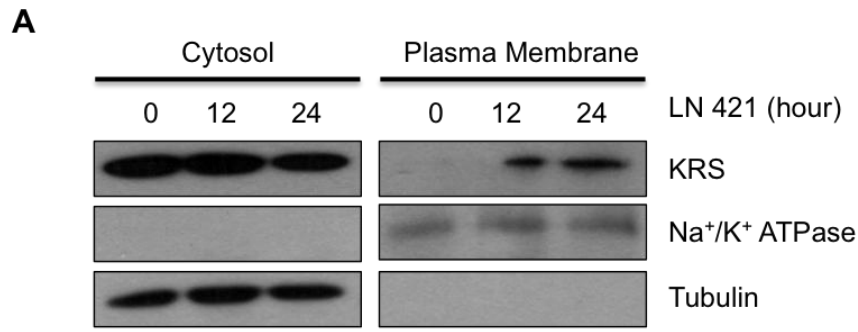

Figure 3. LN 421 signal induces the translocation of KRS to plasma membrane

(A) After 12 hours of cell seeding on 100 mm dish plates (2 x 10^6 seeding), RAW 264.7 cells were treated with LN 421 (1 μg/ml) and incubated for the indicated time (12 hours and 24 hours). Whole cell lysates were fractionated into cytosol and plasma membrane, and the level of KRS in each cellular location was detected by immunoblotting.

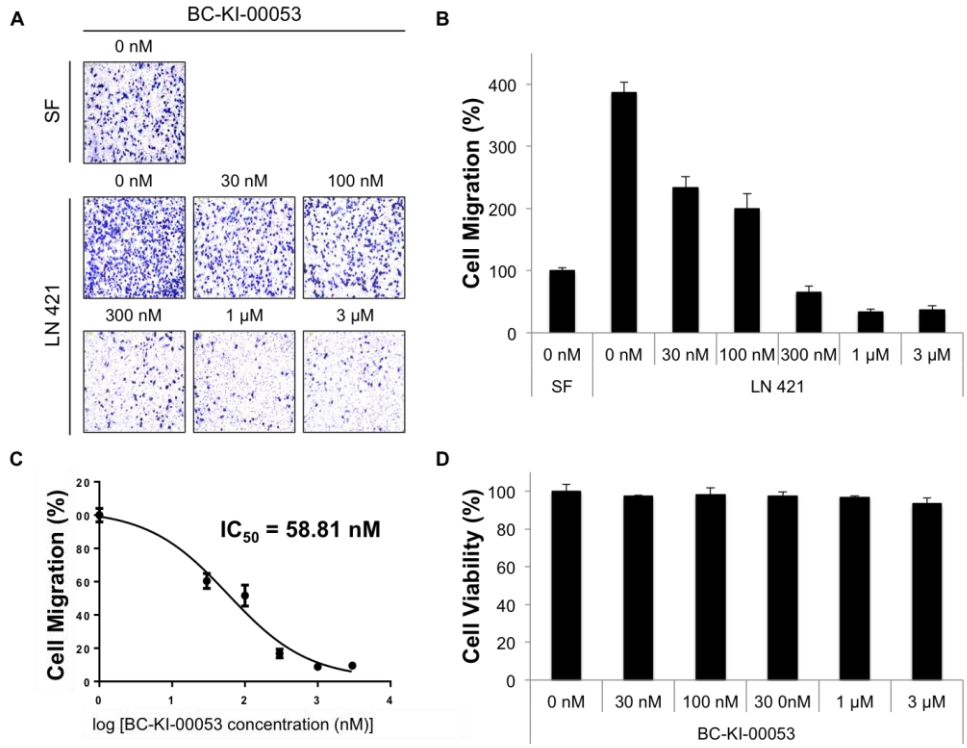

Figure 4. KRS inhibitor (BC-KI-00053) attenuates LN 421-dependent migration of macrophage

(A) RAW 264.7 cells were treated with BC-KI-00053 in a dose dependent manner in the presence of LN 421 (1 μg/ml) and the level of migration was analyzed by staining of the cells with hematoxylin solution.

(B) The number of migrated cells per field was counted and presented as bar graphs (mean ± SD, n = 3).

(C) The anti-migratory effect of BC-KI-00053 on RAW 264.7 cells was analyzed by multi-dose transwell assay and the IC_{50} value of BC-KI-00053 was calculated as 58 nM (mean ± SD, n = 3).

(D) RAW 264.7 cells were treated with BC-KI-00053 (0, 30 nM, 100 nM, 300 nM, 1 μM, and 3 μM) for 24 hours, and cell viability assay was performed using CCK-8 reagent (mean ± SD, n = 3).

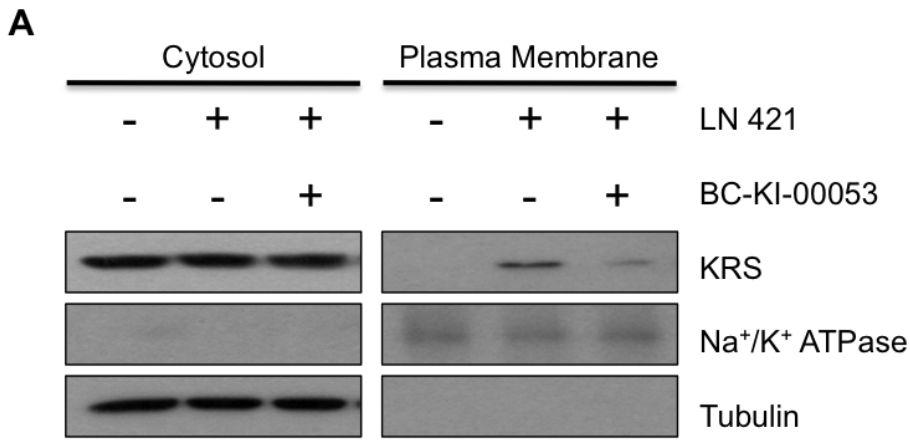

Figure 5. BC-KI-00053 suppresses LN 421-mediated membrane localization of KRS

(A) RAW 264.7 cells were incubated in the presence of LN 421 for 24 hours, and treated with 100 nM of BC-KI-00053 for 4 hours before harvest. Cellular proteins were subjected to fractionation and the level of KRS was determined using immunoblotting. Na^+/K^+ ATPase and tubulin were used as a positive cellular marker of plasma membrane and cytosol, respectively.

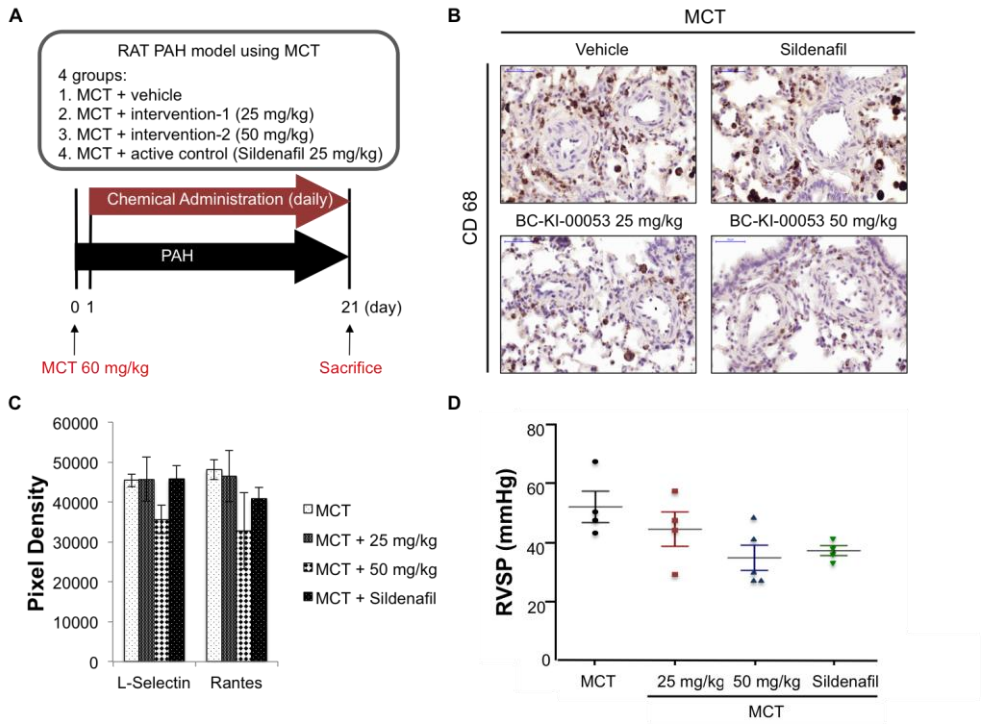

Figure 6. KRS inhibitor (BC-KI-00053) relieves the symptoms of PAH *in vivo*

(A) Schematic depiction of the experimental protocol is presented. Rats were divided into 4 groups: Vehicle treatment, BC-KI-00053 treatment (25 mg/kg), BC-KI-00053 treatment (50 mg/kg), and sildenafil treatment (25 mg/kg). MCT was administered once at day 0, and other chemicals were administrated daily until day 21.

(B) Immunohistochemistry (IHC) staining of rat lung sections was performed with anti-CD 68 antibody to detect monocyte/macrophage.

(C) Rat cytokine array was performed with the sera obtained at day 21. Bar diagrams represent means ± S.E.M pixel densities of the immunoblots.

(D) MCT-injected rats treated with BC-KI-00053 alleviated the PAH symptom as indicated based on the decrease of RVSP in a dose dependent manner. Sildenafil was used as a positive control.

	MCT (n = 4)	MCT + Tx 25 (n = 4)	MCT + Tx 50 (n = 5)	MCT + Sil (n = 4)
RVSP (mmHg)	**51.8 ± 10.6**	**44.3 ± 11.6**	**34.6 ± 9.4***	**37.0 ± 3.4***
CO (ml/min)	60.5 ± 11.4	64.0 ± 8.6	68.3 ± 3.5	60.5 ± 8.6

MCT; monocrotaline, Tx 25; BC-KI-00053 mg/kg, Tx 50; BC-KI-00053 mg/kg, Sil; Sildenafil 25 mg/kg, RVSP; right ventricular end-systolic pressure, and CO; cardiac output. *p <0.05

Table 1. BC-KI-00053 decreases RVSP substantially in MCT-induced rat models

Schematic RVSP of each Rat groups was measured. Compared to MCT-induced rats, group of BC-KI-00053 treatment showed decreased RVSP, but no effect in cardiac output (CO).

DISCUSSION

PAH, a progressive disease characterized by high pulmonary artery pressure, is a relatively rare disease but there is a clear unmet need for the development of effective drugs due to the poor prognosis and side effects of existing drugs (2). In addition, the contribution of inflammatory responses is considered to be the central cause of the proliferation of endothelial cells and smooth muscle cells that participates in the pathology of PAH (17). Macrophages are in charge of the recruitment of other immune cells in the injured area, and exacerbate the inflammation response, fibrosis and tissue damage persisting the symptoms of PAH including hypertension. Despite the high mortality rate due to right heart failure, FDA approved drugs, majorly focusing on the vessel dialysis, are not efficient to halt the progression of PAH. In addition, the approved drugs have various drawbacks such as side effects and limited combination therapy, showing that a novel drug is desperately required to improve patients' survival and quality of life.

In the previous reports, variability in the endothelial basement membrane composition in lung has been observed in pulmonary arterial hypertension, and temporal alterations in laminin were also observed in the model of PAH (10). Laminin α4 such as LN 411 and LN 421 in the endothelial basement membrane is reported as a contributor of cell migration (18). That would be the reason that the membrane localization of KRS, which induces the cell migration in response to laminin stimulus, can facilitate the infiltration of macrophages to the damaged site

in PAH model.

Laminin α4, ubiquitously localized in the endothelial basement membranes, has a decisive role in controlling of immune cell infiltration. While cell migration occurs at regions of basement membrane where laminin α4 is present, other laminin subtypes such as laminin α5 have a inhibitory effect of cell migration (11). In our study, LN 421 triggered the cell migration the most compared to other laminin isoforms (Fig 1), and the functional role of KRS in macrophage migration was also confirmed through western blot *in vitro* (Fig 2). LN 411 is also known as a trigger of immune cell infiltration, but it seems unrelated to the KRS-dependent migration of RAW 264.7 cells. Although this study focused on the LN 421-dependent migration of macrophages and the role of KRS, other immune cells except for macrophages may respond to LN 411. The relationship between laminin subtypes and other immune cells as well as their dependence on KRS for the migration should be further investigated (Fig 3).

BC-KI-00053 effectively decreased the level of KRS in plasma membrane and also inhibited the macrophage migration with IC_{50} value of 55.81 nM without any toxicity (Fig 4 and Fig 5). It coincides with the anti-migratory effect of BC-KI-00053 in cancer cells proving that the mode of action of this compound is the same regardless of cell types. The working mechanism of BC-KI-00053 was confirmed again in vivo PAH model (Fig 6), showing the substantially reduced macrophage infiltrated in lung tissue with the relieved symptoms of PAH.

Cytokine array was performed to monitor the change of cytokines and chemokines involved in the PAH-responsive immune reaction. According to the cytokine array results, Rantes, known as important biomarkers in severe PAH (19)

and L-selectin, inducer of monocyte and macrophage infiltration, were respectively reduced by BC-KI-00053 in a does dependently (20). Given that BC-KI-00053 seemingly downregulated pulmonary vascular resistance, it implies that the control of KRS-mediated macrophage infiltration would be a good strategy to regulate the reactive immune responses as well as the following hypertension. It is interesting that BC-KI-00053 can effectively reduce the RVSP value at a similar level like Sildenafil, which is a potent vasodilator. Considering this result, BC-KI-00053 can be plausibly applicable to other diseases related to excessive macrophage infiltration that is critical for the development of fibrosis and hypertension.

In this study, we investigated and proved the functional role of KRS in the pathology of PAH. We suggested a novel mechanism of KRS involved in the macrophage migration, and BC-KI-00053 as an effective lead for the treatment of PAH. Although additional evidences pertaining in the signaling pathway of KRS-laminin should be further evaluated, it is worth noting that KRS inhibition can be a good strategy to control PAH achieving the clinical unmet need.

REFERENCES

1. Luster AD, Alon R, & von Andrian UH (2005) Immune cell migration in inflammation: present and future therapeutic targets. Nat Immunol 6(12):1182-1190.
2. Chelladurai P, Seeger W, & Pullamsetti SS (2012) Matrix metalloproteinases and their inhibitors in pulmonary hypertension. Eur Respir J 40(3):766-782.
3. Sparacino-Watkins CE, Lai YC, & Gladwin MT (2012) Nitrate-nitrite-nitric oxide pathway in pulmonary arterial hypertension therapeutics. Circulation 125(23):2824-2826.
4. Quittner AL, et al. (2014) Pulmonary medication adherence and health-care use in cystic fibrosis. Chest 146(1):142-151.
5. de Jesus Perez V, Yuan K, Alastalo TP, Spiekerkoetter E, & Rabinovitch M (2014) Targeting the Wnt signaling pathways in pulmonary arterial hypertension. Drug Discov Today 19(8):1270-1276.
6. Vergadi E, et al. (2011) Early macrophage recruitment and alternative activation are critical for the later development of hypoxia-induced pulmonary hypertension. Circulation 123(18):1986-1995.
7. Jonigk D, et al. (2011) Plexiform lesions in pulmonary arterial hypertension composition, architecture, and microenvironment. Am J Pathol 179(1):167-179.
8. Thenappan T, et al. (2011) A central role for CD68(+) macrophages in hepatopulmonary syndrome. Reversal by macrophage depletion. Am J Respir Crit Care Med 183(8):1080-1091.
9. Rubin LJ (2002) Therapy of pulmonary hypertension: the evolution from vasodilators to antiproliferative agents. Am J Respir Crit Care Med 166(10):1308-1309.

10. Vyas-Somani AC, et al. (1996) Temporal alterations in basement membrane components in the pulmonary vasculature of the chronically hypoxic rat: impact of hypoxia and recovery. Am J Med Sci 312(2):54-67.

11. Sorokin L (2010) The impact of the extracellular matrix on inflammation. Nat Rev Immunol 10(10):712-723.

12. Soon E, et al. (2010) Elevated levels of inflammatory cytokines predict survival in idiopathic and familial pulmonary arterial hypertension. Circulation 122(9):920-927.

13. Kim S, You S, & Hwang D (2011) Aminoacyl-tRNA synthetases and tumorigenesis: more than housekeeping. Nat Rev Cancer 11(10):708-718.

14. Park SG, Schimmel P, & Kim S (2008) Aminoacyl tRNA synthetases and their connections to disease. Proc Natl Acad Sci U S A 105(32):11043-11049.

15. Kim DG, et al. (2012) Interaction of two translational components, lysyl-tRNA synthetase and p40/37LRP, in plasma membrane promotes laminin-dependent cell migration. FASEB J 26(10):4142-4159.

16. Kim DG, et al. (2014) Chemical inhibition of prometastatic lysyl-tRNA synthetase-laminin receptor interaction. Nat Chem Biol 10(1):29-34.

17. Huertas A, et al. (2014) Immune dysregulation and endothelial dysfunction in pulmonary arterial hypertension: a complex interplay. Circulation 129(12):1332-1340.

18. Ishikawa T, et al. (2014) Laminins 411 and 421 differentially promote tumor cell migration via alpha6beta1 integrin and MCAM (CD146). Matrix Biol 38:69-83.

19. Dorfmuller P, et al. (2002) Chemokine RANTES in severe pulmonary arterial hypertension. Am J Respir Crit Care Med 165(4):534-539.

20. Unver N, Esendagli G, Yilmaz G, & Guc D (2015) CXCL7-induced macrophage infiltration in lung tumor is independent of CXCR2 expression: CXCL7-induced macrophage chemotaxis in LLC tumors. Cytokine 75(2):330-337.

21. Imhof BA & Aurrand-Lions M (2004) Adhesion mechanisms regulating the migration of monocytes. Nat Rev Immunol 4(6):432-444.

요약 (국문초록)

대식세포의 움직임을 조절하는 Lysyl-tRNA Synthetase (KRS)의 기전 연구

서울대학교
융합과학기술대학원
분자의학 및 바이오제약학과 의약생명과학전공
김건호

면역세포의 움직임과 관련된 염증반응이 사람의 질병과 깊게 연관이 있다는 사실이 밝혀지면서 질병을 치료하기 위한 방식으로서의 면역 연구에 대한 관심이 증대되어 왔다. 면역세포의 움직임은 병원균으로부터 몸을 보호하는데 중요한 역할을 하지만 과도한 면역세포의 움직임에 따른 비정상적인 신호전달은 여러 질병을 유발시킨다. 그 중에서도 폐동맥 고혈압 (Pulmonary arterial hypertension) 은 면역세포의 침윤이 병리적으로 중요한 대표적인 질병이다. 하지만 현재 사용되는 치료제들은 대증치료에 집중되어 있고 부작용이 심해 보다 근본적인 치료법이 요구되고 있다. 본 연구에서는 아미노아실 tRNA 합성효소 (Aminoacyl tRNA synthetases, ARSs) 중 하나인 라이실 tRNA 합성효소 (Lysyl-tRNA synthetase, KRS)의 조절을 통해 폐동맥 고혈압을 조절할 수 있음을 밝혔

다. KRS는 라미닌 신호에 의해 세포막으로 이동, 암전이 (cancer metastasis)에서 중요한 역할을 한다고 알려져 있으나 면역세포의 이동과 관련된 정확한 역할은 아직 알려져 있지 않다.

본 연구를 통해 KRS가 대식세포의 이동을 촉진하는 중요한 요소이며 KRS의존적인 대식세포 이동 조절을 통해 폐동맥 고혈압을 완화시킬 수 있음을 시험관 내 (*in vitro*) 실험 및 생체 내 (*in vivo*) 실험을 통하여 증명하였다. 특히 라미닌 (laminin) 421이 KRS 의존적인 대식세포 이동을 유도하는 주요 세포외기질임을 밝혔으며 라미닌 421 처리에 의해 KRS의 세포막이동이 대식세포에서 촉진됨을 확인하였다. 암세포이동을 저해하는 KRS 억제제 BC-KI-00053 화합물 처리를 통해 대식세포에서의 KRS 세포막 수준 감소 및 면역세포의 이동 감소 효과를 확인하였다. BC-KI-00053 처리는 monocrotaline 폐동맥고혈압 동물모델에서도 폐로의 대식세포 침윤을 현저히 저해하였고 관련 사이토카인의 감소를 유도하였으며 우심실 수축기 혈압 (right Ventricular Systolic Pressure)을 완화하였다.

결론적으로 본 연구를 통해 KRS가 대식세포의 움직임을 조절하는 중요한 조절인자임을 밝혔으며 폐동맥 고혈압 치료를 가능하게 할 우수한 표적인자임을 제시하였다.

주요어 : 라이실 tRNA 합성효소, 대식세포, 이동, 억제, 라미닌, 폐동맥 고혈압

학 번 : 2015-26071